



City Research Online

City, University of London Institutional Repository

Citation: Lungu, A. and Giaralis, A. (2013). A non-separable stochastic model for pulse-like ground motions. Paper presented at the 11th International Conference on Structural Safety and Reliability for Integrating Structural Analysis, Risk and Reliability, 16 - 20 June 2013, New York, USA.

This is the unspecified version of the paper.

This version of the publication may differ from the final published version.

Permanent repository link: <http://openaccess.city.ac.uk/2812/>

Link to published version:

Copyright and reuse: City Research Online aims to make research outputs of City, University of London available to a wider audience. Copyright and Moral Rights remain with the author(s) and/or copyright holders. URLs from City Research Online may be freely distributed and linked to.

City Research Online:

<http://openaccess.city.ac.uk/>

publications@city.ac.uk

A non-separable stochastic model for pulse-like ground motions

A. Lungu & A. Giaralis

City University London, United Kingdom

ABSTRACT: A phenomenological non-separable non-stationary stochastic model is proposed to represent near-fault pulse-like ground motions (PLGMs) by means of a parametrically defined evolutionary power spectrum (EPSD). Numerical data pertaining to ensembles of EPSD compatible realizations and considering statistical analysis of peak elastic and inelastic spectral ordinates demonstrate the applicability of the model to capture the salient effects of PLGMs to structural responses. To this aim, the model parameters are calibrated against a field recorded PLGM. Further numerical data considering stochastic processes compatible with the response spectrum of the European aseismic code (EC8) are furnished to demonstrate the potential of the proposed model for including near-fault effects to spectrum compatible representations of the seismic action. It is foreseen that this model can be a useful tool in accounting for the low-frequency content of PLGMs in both Monte Carlo simulation-based analyses and in statistical linearization based studies.

1 INTRODUCTION

Civil structures located in the proximity of seismic faults are expected to experience a number of high intensity strong ground motions (GMs) during their life-time. Seismological considerations and statistical signal analysis of databanks of recorded accelerograms suggest that, under certain conditions, near-fault GMs may be characterized by one or more long-period high-amplitude pulse(s) (e.g. Mavroeidis & Papageorgiou 2003, Baker 2007, Moustafa & Takewaki 2010, Vasiliou & Makris 2011). It has been observed in recorded "pulse-like ground motions" (PLGMs) that, in many cases, such low frequency pulses carry a significant fraction of the total energy carried by GM signal traces. Consequently, compared with typical far-field GMs, PLGMs impose higher ductility demands to relatively flexible structures, with periods close to the dominant period of the pulse(s).

In this regard, it is important to account for the effects of PLGMs in the aseismic design of new relatively flexible structures and in assessing the seismic vulnerability of the existing ones in near-fault environments (e.g. He & Agrawal 2008, Sehhati et al. 2011, Taflanidis & Jia 2011). To facilitate this aim, considerable research effort has been devoted to modeling and simulation of PLGMs. In doing so, the higher frequency (HF) content and the low-frequency (LF) content in PLGM models are considered separately. Commonly, the HF content is mod-

eled by standard approaches used for modeling and simulating pulse-free GMs (e.g. Mavroeidis & Papageorgiou 2003, Fu & Menun 2004, Dickinson & Gavin 2011, Dabaghi et al. 2011). Further, with very few exceptions (e.g. Moustafa & Takewaki 2010), the LF content of PLGM models is defined in the time-domain by means of parametrically defined "pulse-like" functions. The assumed analytical expressions for these functions take the form of simple waveforms (e.g. Alavi & Krawinkler 2001) or of more involved oscillatory functions with decaying envelopes: "wavelets" (e.g. Mavroeidis & Papageorgiou 2003, He & Agrawal 2008, Moustafa & Takewaki 2010, Dickinson & Gavin 2011). The underlying parameters used to define these functions are related to salient pulse features such as the pulse peak value (amplitude) and its time location, the "dominant" pulse frequency or period, and the number of pulse cycles (oscillations). These parameters are obtained by "fitting" operations to field recorded GMs (e.g. Mavroeidis & Papageorgiou 2003, Dickinson & Gavin 2011) or by joint time-frequency signal analyses techniques used as "matched filtering" tools to detect/extract pulses from recorded GMs. For instance, Baker (2007) has considered the application of the discrete wavelet transform using a Daubechies wavelet family for pulse identification, extraction, and characterization, while Vasileiou and Makris (2012) considered a heuristic form of the Gaussian chirplet transform for the purpose (see Spanos et al. 2007 and references therein).

In accounting for the observed variability in the properties of pulses extracted from recorded PLGMs, several researchers have considered the treatment of the parameters of the considered pulse-like functions to represent the LF content of PLGMs as random variables within a Monte Carlo simulation based framework (see e.g. Taflanidis & Jia 2011, Dabaghi et al. 2011). Nevertheless, the statistical properties for only some of the commonly considered pulse parameters have been estimated by regression analyses to pulses extracted by certain databanks of recorded PLGMs. As such databanks are currently not very well populated and do not cover all possible “scenario seismic events” this probabilistic approach to model the uncertainty of the LF content in PLGMs may not be possible in practical applications. In this respect, an alternative probabilistic model has been proposed by Moustafa & Takewaki (2010), who represented the pulses in the frequency domain by means of “delta functions”. However, the latter representation allows for limited flexibility to realistically capture the diversity of the frequency content of the pulses observed in PLGMs.

In this work, a novel PLGM stochastic model is proposed which treats the inclusion of the LF content to the typical HF content of GMs as a “low-frequency enrichment” step of the energy distribution of the acceleration stochastic processes on the time-frequency plane. This model circumvents some of the aforementioned limitations of the stochastic PLGM models found in the literature while it aims to simplicity and to “ease of use”. From the physics viewpoint, the proposed model is motivated by the fact that recorded pulse-like accelerograms are characterized by prominent low-frequency “bursts of energy” on the time-frequency plane as captured by wavelet transform-based kinds of analyses (Giaralis and Lungu 2012). From the structural analysis viewpoint, this model can be readily used not only for simulation based analyses (e.g. Taflanidis and Jia 2011), but also in conjunction with non-linear stochastic dynamics techniques, such as statistical linearization (see e.g. Spanos & Kougioumtzoglou 2011). In particular, the considered PLGM model is defined as the superposition of amplitude modulated zero-mean uncorrelated acceleration stationary random processes characterizing separately the HF and the LF content (see also Conte & Peng 1997, Spanos & Failla 2004). Appropriate parametric expressions are used to define the frequency content and time-evolving intensity of the considered separable evolutionary random processes. Pertinent numerical results are included to illustrate the calibration of the model parameters against a specific field recorded pulse-like accelerogram. Further, linear and non-linear response spectra are considered to assess the effectiveness of the model to capture the structural impact/damage potential in a simulation-based context. Finally, the versatility of the proposed model to

incorporate near-field effects (pulses) in code-compliant response spectrum compatible stochastic representations is also discussed in view of numerical data considering the response/design spectrum of the current European aseismic code (CEN 2004).

2 STOCHASTIC MODEL FOR PLGMS

Consider the non-separable non-stationary stochastic process expressed by

$$y(t) = y_{HF}(t) + y_{LF}(t) = a_{HF}(t)g_{HF}(t) + a_{LF}(t)g_{LF}(t) \\ = \sum_{r=1}^2 a_r(t)g_r(t), \quad (1)$$

where y_{HF} and y_{LF} are independent evolutionary stochastic processes of the separable kind. Specifically, each of these processes are defined by a stationary zero-mean random process $g_r(t)$, uniformly modulated by a deterministic time-varying envelope function $a_r(t)$. It can be shown that for envelop functions $a_r(t)$ which vary sufficiently slowly in time, the energy distribution of the process $y(t)$ on the time-frequency plane can be represented by the concept of the evolutionary power spectrum (EPSD), given by the expression (Priestley 1965, Conte & Peng 1997)

$$S(t, \omega) = |a_{HF}(t)|^2 G_{HF}(\omega) + |a_{LF}(t)|^2 G_{LF}(\omega) \\ = \sum_{r=1}^2 |a_r(t)|^2 G_r(\omega). \quad (2)$$

In the above equation, $G_r(\omega)$ denotes the power spectrum density function characterizing the stationary random process $g_r(t)$ in the frequency domain.

It is noted that EPSDs of the form of Equation 2, assuming appropriately defined analytical expressions for the envelope function a_r and the power spectrum G_r , have been extensively used in the literature for the stochastic modeling of the earthquake induced acceleration trace of strong ground motions. For instance, Spanos & Vargas Loli (1985) have considered the stochastic model of Equation 2 for the generation of artificial spectrum compatible accelerograms in a stochastic framework. Conte & Peng (1997) have used the aforementioned model for the characterization and representation of certain field recorded accelerograms associated with specific historic seismic events. More recently, Spanos & Failla (2004) considered ensembles of seismic accelerograms compatible with an EPSD of the form of Equation 2 to assess the potential of the wavelet transform to characterize the underlying evolutionary frequency content of non-stationary processes in a Monte Carlo based context.

Herein, the non-stationary stochastic process of Equation 1 is used to represent the acceleration trace of PLGMs. This is achieved by defining the HF and the LF content of the PLGMs, corresponding to the $y_{HF}(t)$ and the $y_{LF}(t)$ processes respectively, separate-

ly as detailed in the remainder of this section. The proposed model assumes that the HF content is represented by methods applicable to modeling far-field GMs and is statistically uncorrelated to the LF pulses observed in PLGMs (“near-fault” effects).

2.1 Definition of the high frequency process y_{HF}

For the purposes of this work, a Clough-Penzien (CP) spectral form is considered to represent the HF content of the proposed model corresponding to the stationary process $g_{HF}(t)$ in Equation 1. Specifically, the CP two-sided power spectrum density with cut-off frequency $\omega_{c,HF}$ is given as (Clough & Penzien 1993)

$$G_{HF}(\omega) = \frac{\left(\frac{\omega}{\omega_f}\right)^4}{\left(1 - \left(\frac{\omega}{\omega_f}\right)^2\right)^2 + 4\zeta_f^2 \left(\frac{\omega}{\omega_f}\right)^2} \times \frac{1 + 4\zeta_g^2 \left(\frac{\omega}{\omega_g}\right)^2}{\left(1 - \left(\frac{\omega}{\omega_g}\right)^2\right)^2 + 4\zeta_g^2 \left(\frac{\omega}{\omega_g}\right)^2}, \quad |\omega| \leq \omega_{c,HF} \quad (3)$$

The first ratio in Equation 3 corresponds to a high-pass filter with a low cut-off frequency ω_f to suppress low frequency components. The ζ_f parameter controls the “slope steepness” of the filter. Both parameters should be chosen to ensure that the HF content of the PLGM model does not “scramble” with the LF content defined by $G_{LF}(\omega)$. In this respect, ω_f and ζ_f does not bear any physical significance (see also Giaralis & Spanos 2009). The second ratio in Equation 3 is the well-known Kanai-Tajimi spectrum which accounts for local site conditions by means of the ω_g and ζ_g parameters. They can be interpreted as the “stiffness” and “damping” of the surface soil layers, respectively (e.g. Lai 1982, Giaralis & Spanos 2009).

The transient time-varying nature of the HF content is accounted for by the exponential envelope function (Bogdanoff et al. 1961)

$$a_{HF}(t) = C_{HF} h_{HF}(t) \quad ; \quad h_{HF}(t) = te^{-\frac{b_{HF}t}{2}} \quad (4)$$

The C_{HF} parameter is proportional to the peak amplitude of the envelope, while the parameter b_{HF} controls its shape (see e.g. Giaralis & Spanos 2009). Spanos et al. (2009) showed that a one-to-one non-linear relationship exists between b_{HF} and the effective duration of the ground motion T_{eff} (Trifunac and Brady 1975) commonly used in earthquake engineering applications (T_{eff} = time interval in which the central 90% of the total energy of the GM is released; see also Giaralis and Spanos 2012).

It is noted in passing that more involved physics-based stochastic models (e.g. Boore 2003) can be readily accommodated by the herein proposed model and be used as surrogates to Equations 3 and 4.

2.2 Definition of the low frequency process y_{LF}

Two different analytical expressions are considered to define the LF content in the proposed PLGM model characterized by the power spectrum $G_{LF}(\omega)$ (Figure 1a,b): a “simple” box-like function (BOX) and a more involved raised cosine function (COS), both centered at ω_p the pulse dominant frequency.

The BOX spectrum is given by the expression

$$G_{LF}^{BOX}(\omega) = \begin{cases} 1, & \text{for } \omega_p - B/2 \leq \omega \leq \omega_p + B/2, \\ 0, & \text{otherwise} \end{cases} \quad (5)$$

where the term B determines the bandwidth of the LF content. The COS spectrum is given as

$$G_{LF}^{COS}(\omega) = \frac{1}{2} \left(1 + \cos \left(\frac{2\pi}{2\alpha\omega_p} (\omega - \omega_p) \right) \right), \quad (6)$$

for $\omega(1-\alpha) \leq \omega \leq \omega(1+\alpha)$

where $\alpha \leq 1$ is a shape parameter (see Figure 1b).

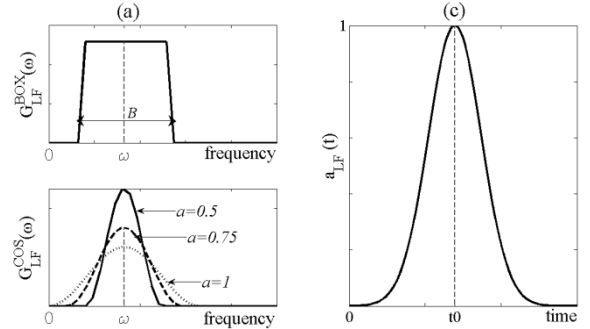


Figure 1 BOX (a) and COS (b) LF power spectra $G_{LF}(\omega)$ and LF envelope function $a_{LF}(t)$ (c).

The transient nature of the pulse-like LF content in the time-domain is accounted for by the envelope function (Figure 1c)

$$a_{LF}(t) = C_{LF} h_{LF}(t) \quad ; \quad h_{LF}(t) = e^{-\frac{\omega_p}{\gamma}(t-t_0)} \quad (7)$$

The parameter C_{LF} is proportional to the peak amplitude of the pulse content. Further, the adopted exponential function $h_{LF}(t)$ involves three parameters ω_p , t_0 , and γ which are commonly used for time-domain pulse characterization (e.g. Mavroeidis & Papageorgiou 2003, Moustafa & Takewaki 2010). In particular, ω_p and t_0 control the shape of the envelope and represent the pulse dominant frequency and the time instant when its peak is attained. Moreover, the $\gamma > 1$ has limited physical significance and should be chosen such that the frequency content of the envelope falls outside the bandwidth spanned by the

$G_{LF}(\omega)$ in the frequency domain (Mavroeidis & Papageorgiou 2003).

3 GENERATION OF PLGMS COMPATIBLE WITH THE STOCHASTIC MODEL

Pulse-like acceleration time-histories compatible with the previously described stochastic model can be readily generated using any qualified technique for stationary power spectrum compatible random field simulation (Spanos and Zeldin 1998). Figure 2 illustrates the steps that need to be taken for the purpose. Non-stationary samples compatible with the HF separable EPSD (Equations 3,4) and LF separable EPSD (Equations 6-8) are generated separately and independently and added together to obtain simulated PLGMS compatible with the non-stationary non-separable EPSD $S(t,\omega)$ of Equation 2.

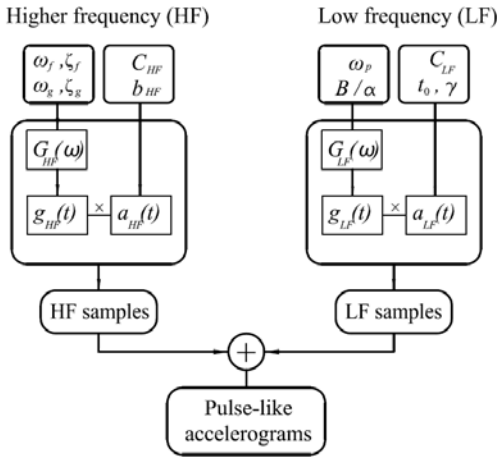


Figure 2 Flowchart for obtaining pulse-like acceleration time-histories compatible with the considered stochastic model.

In all the ensuing numerical results, the spectral representation method is employed to generate uniformly modulated samples in two steps. First, stationary samples compatible with the $G_r(\omega)$ spectra are generated as a sum of appropriately scaled harmonically related cosines with uniformly distributed on the $[0,2\pi)$ interval random phases Φ_n (Shinozuka & Deodatis 1991). Specifically, a discrete-time sample $g_r[k] = g_r(k\Delta t)$, $k=0,1,\dots,M-1$ is computed as

$$g_r[k] = 2 \sum_{n=0}^{N-1} \sqrt{G_r(n\Delta\omega)} \Delta\omega \cos(n\Delta\omega k\Delta t + \Phi_n). \quad (8)$$

This is a T_0 -periodic sample with $T_0=M\Delta t$. Further, $\Delta t \leq \pi/\omega_c$ is the time-domain discretization step with ω_c being the cut-off frequency of the $G_r(\omega)$ spectrum, and $\Delta\omega=2\pi/T_0$ is the frequency-domain discretization step. Note that uncorrelated vectors of random phases Φ_n have to be generated for each sample to ensure that the HF and LF time-histories are uncorrelated. Next, the thus generated HF and LF stationary samples are multiplied by the corresponding envelop functions g_r and added (Figure 2).

4 MODEL CALIBRATION AND STRUCTURAL RESPONSE ASSESSMENT FOR A RECORDED PLGM

In this section the versatility of the stochastic model defined in section 2 to capture PLGMS and to represent their structural damage potential is illustrated by considering a field recorded accelerogram classified in Baker (2007) as a PLGM, namely the El Centro array #6 component of the 1999 Imperial Valley earthquake. The acceleration trace $a_g(t)$ of this record is plotted in Figure 3, along with its low-frequency pulse $p(t)$ extracted by Baker (2007) using the discrete wavelet transform. The HF residual $r(t) = a_g(t) - p(t)$ is also plotted in the same figure. In the next sub-section the above pulse and residual time-histories are considered to calibrate the parameters of the stochastic model presented in section 2.

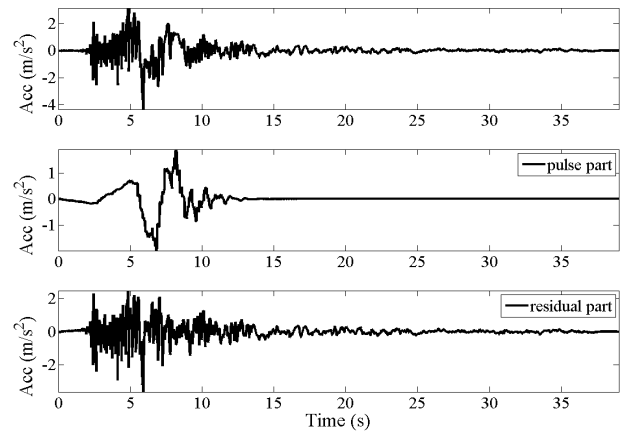


Figure 3 Acceleration trace, LF pulse, and HF residual trace of the El Centro array #6- 1999 Imperial Valley earthquake. http://www.stanford.edu/~bakerjw/pulseclassification_old.html

4.1 Stochastic model parameter calibration

A total number of 11 parameters are required to fully define the PLGM model of section 2. The definition of the HF content involves 6 parameters (4 for the G_{HF} function and 2 for the a_{HF} function), while the LF content involves 5 parameters (2 for the G_{LF} function and 3 for the a_{LF} function)

The parameters for defining the power spectrum of the HF content are obtained by fitting the C-P spectrum of Equation 3 to the squared Fourier transform of the residual time-history, shown in Figure 3, using standard nonlinear least squares regression. The initial guess for the parameters characterizing the soil conditions (ω_g and ζ_g) are provided using the empirical formulations given by Lai (1982).

Two alternative spectral forms have been proposed to define the power spectrum of the LF content: Equation 5-BOX and Equation 6-COS. The parameter ω_p (pulse dominant frequency) appearing in both of them is taken equal to $2\pi/T_p$ where T_p is the pulse period estimated by Baker (2007). Further, for the BOX spectrum, the bandwidth B parameter is

taken equal to its ω_p , while for the COS spectrum the shape parameter α is taken equal to 0.50.

The parameter estimation for the definition of the modulating functions $a_{HF}(t)$ and $a_{LF}(t)$ is achieved by first considering the envelopes of the residual and of the extracted pulse shown in Figure 3. Following the standard analytic signal theory, these envelopes are derived by using the expression (Dugundji 1958)

$$e(t) = \sqrt{s^2(t) + H(s(t))^2} \quad (9)$$

where $H(\cdot)$ denotes the Hilbert transform and s stands for “signal”. The pulse $p(t)$ and the residual $r(t)$ take the place of the signal in the above equation to obtain the envelopes $e_p(t)$ and $e_r(t)$, respectively. Next, the functions defined in Equations 4 and 7 are fit to the above estimated envelopes, respectively. In fitting $a_{HF}(t)$, the parameter b_{HF} is treated as a constant whose value is estimated based on the effective duration T_{eff} of the residual.

Table 1 reports the values of all 11 parameters used to calibrate the proposed stochastic model against the recorded PLGM of Figure 3. In the next sub-section the potential of the calibrated model to capture the salient features of the considered PLGM in terms of peak structural responses is assessed.

Table 1. Parameter calibration of the PLGM model to represent the recorded accelerogram of Figure 3.

High-frequency content	$a_{HF}(t)$	$C_{HF} = 0.53$
		$b = 0.5 \quad (s^{-1})$
	$G_{HF}(\omega)$	$\zeta_f = 0.55$
		$\omega_f = 2.33 \quad (\text{rad/s})$
$\omega_g = 21 \quad (\text{rad/s})$		
Low-frequency content	$a_{LF}(t)$	$C_{LF} = 1.65 \quad (\text{m/s}^2)$
		$\omega_p = 1.65 \quad (\text{rad/s})$
	$\gamma = 2.89$	
	$t_0 = 6.96 \quad (\text{s})$	
	$G_{LF}(\omega)$	BOX $\omega_p = 1.65 \quad (\text{rad/s})$
COS $B = 1.65 \quad (\text{rad/s})$ $\alpha = 0.50$		

4.2 Model verification via Monte Carlo analysis for linear and inelastic peak structural response

Ensembles of 200 realizations, compatible with each of the three separable EPSDs defined in Table 1 (HF- Equations 3 and 4; BOX (LF)- Equations 5 and 7; COS (LF)- Equations 6 and 7), are generated using the spectral representation method briefly reviewed in section 3. Each realization has a duration of 40s and a time step of 0.005s. These signals are base-line adjusted by acausal forward/backward high-pass filtering using a Butterworth filter to remove spurious low-frequency trends yielding unrealistic velocity and/or displacement traces (see also Giaralis and Spanos 2009 and therein references).

Lastly, the LF samples are added to the HF samples to obtain two different ensembles (HF+BOX and HF+COS) of 200 simulated pulse-like accelerograms each. An arbitrary accelerogram belonging to the HF+BOX ensemble and its velocity and displacement traces is shown in Figure 4.

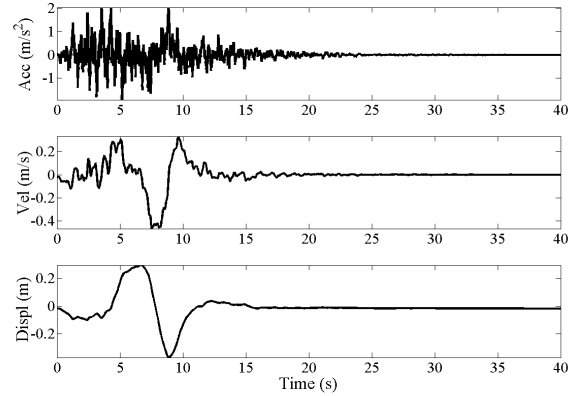


Figure 4 Sample of the HF+BOX process generated for the simulation of the Imperial Valley record

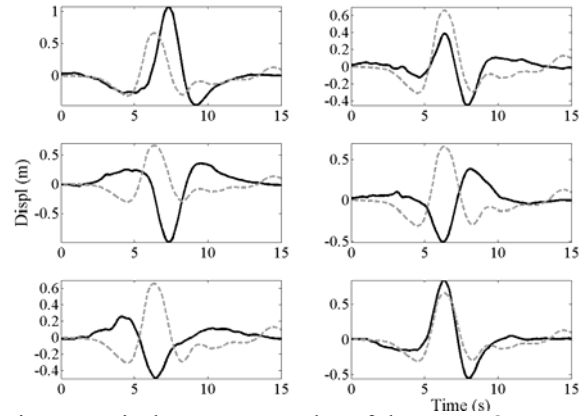


Figure 5 Displacement samples of the HF+BOX process (solid line) and the Imperial Valley displacement (dashed line)

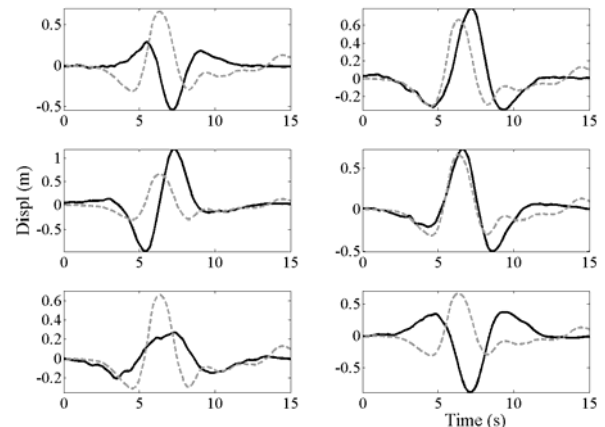


Figure 6 Displacement samples of the HF+COS process (solid line) and the Imperial Valley displacement (dashed line)

Focusing on the detrimental LF content of the considered PLGM model, Figures 5 and 6 plot displacement traces of several arbitrarily chosen accelerograms of the HF+BOX and the HF+COS ensembles, respectively. From a signal processing view point, these time-histories represent low-pass filtered versions of the acceleration traces (Worden 1990), and, thus, they characterize the LF pulse-like

content of the signals in the time-domain. Superimposed on the above two figures is the displacement trace of the El Centro array #6 recorded PLGM to allow for a qualitative comparison between the original and the simulated signals. It can be seen that the time-domain traces of the LF “pulse-like” content, as captured in the displacement time-histories, varies across the realizations of the two generated ensembles in terms of its peak value, of the time instant that this value is attained, of the number oscillations, etc. However, *on the average*, the LF content of the simulated signals approximate well the displacement time-history of the “target” recorded signal while they resemble LF content observed/extracted in recorded PLGMs (see e.g. Mavroeidis & Papageorgiou 2003, Baker 2007, Moustafa & Takewaki 2010). The above qualitative observations verify the usefulness and applicability of the considered stochastic model to generate realistic PLGM time-histories which further bring about a desirable level of “randomness” within a Monte Carlo analyses context.

Furthermore, Figures 7-9 furnish data in terms of peak elastic and inelastic response spectral ordinates to assess the potential of the HF+BOX and HF+COS models of Table 1 to yield structural responses comparable to those obtained by the recorded PLGM considered to “calibrate” these stochastic models. Specifically, Figure 7 include elastic response spectral statistics for 5% critical damping ratio derived from the HF+BOX and HF+COS ensembles (200 realizations each) together with the elastic response spectra of the recorded PLGM of Figure 4. Further, Figure 8 includes similar plots in terms of constant ductility ($\mu=2$) inelastic spectral ordinates assuming critically damped to 5% bilinear hysteretic oscillators with pre/post-yielding stiffness ratio equal to 5%. Finally, Figure 9 plots the mean values of the response spectral ordinates of the HF+BOX and HF+COS ensembles including in the previous two figures normalized to the corresponding response spectral ordinates of the considered “target” recorded PLGM according to the ratio (see also Fu and Menun 2004)

$$\psi(T, \mu) = \frac{E[S_d^{simulated}(T)]}{S_d^{recorded}(T)} \quad (10)$$

Overall, the average peak responses for both the ensembles considered compatible with the calibrated HF+BOX and HF+COS processes of Table 1 compare reasonably well with the “target” values of the recorded PLGM of Figure 4. In the range of long periods (greater than 2s) better agreement is observed for the elastic response spectra considered, though in all cases the average spectral ordinates “fluctuate” about the target value well within the plus/minus one standard deviation interval. More importantly, practically insignificant differences are observed in terms of peak structural response data derived by the

two alternative spectral forms used to represent the LF content (Equations 6 and 7). This observation suggests that the shape of the spectral form adopted to model the LF content may not be an influential factor in the use of the model as input for structural analyses.

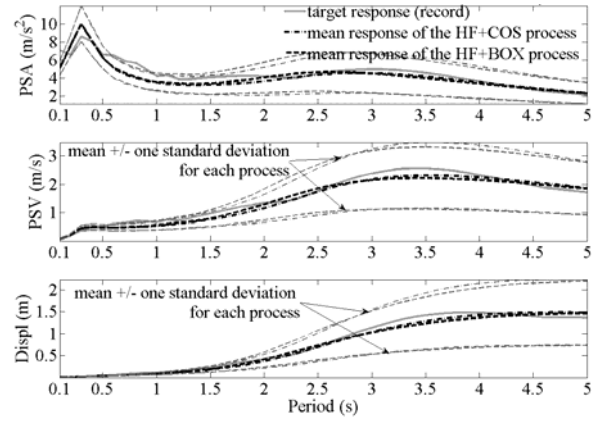


Figure 7 Statistics of elastic response spectral ordinates of the HF+BOX and HF+COS processes (Table 1)- 200 realizations

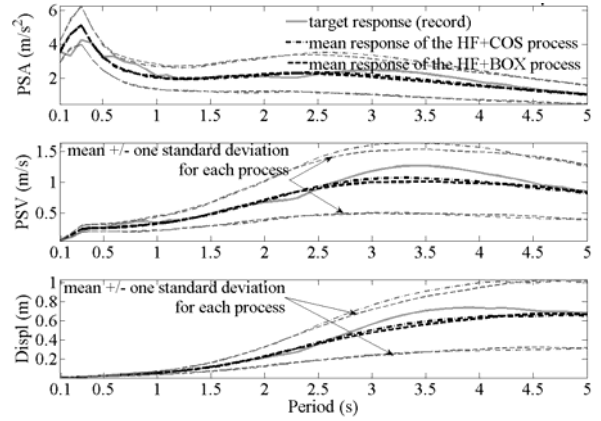


Figure 8 Statistics of constant ductility ($\mu=2$) inelastic response spectral ordinates of the HF+BOX and HF+COS processes (Table 1)- 200 realizations.

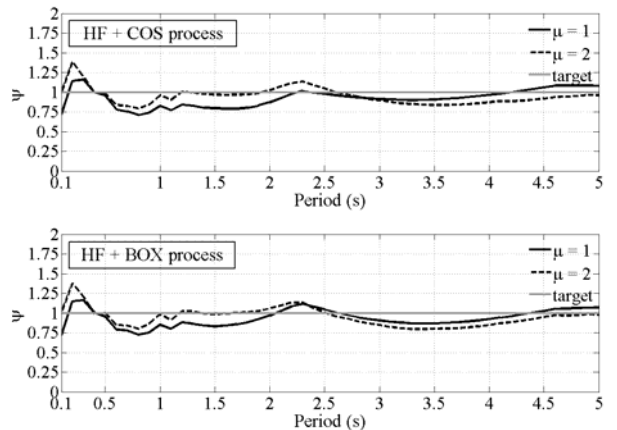


Figure 9 Response ratios ψ (Equation 10) for the HF+COS and HF+BOX processes (Table 1)- 200 realizations.

Further, for structures of shorter fundamental natural periods (less than 2s) whose peak response is dominated by the HF content, larger discrepancies are observed, partly due to the relatively simplistic HF spectral model adopted in this numerical study. This issue can be readily rectified, if so desired, by

adopting HF spectral models incorporating more “degrees of freedom” to achieve a better fit to recorded GMs (see e.g. Conte & Peng 1997, Boore 2003). Such spectra can be readily accommodated by the PLGM model of Equation 1. The next section furnishes further numerical results associated with the use of HF spectral shapes compatible with the response/design spectrum of the European aseismic code- EC8.

5 GENERATION OF PLGMS COMPATIBLE WITH THE EC8 SPECTRUM

This section illustrates the applicability of the proposed PLGM model of section 2 to represent code-compliant response spectrum compatible seismic excitations in which accounting for pulse-like LF content is deemed essential. To this aim, a C-P evolutionary power spectrum compatible with the elastic response spectrum of the European EC8 aseismic code (CEN 2004) is adopted to represent the HF content of the PLGM model (Giaralis & Spanos 2012). The parameters used to define the HF content are reported in Table 2. The LF processes derived in the previous section are considered to define the LF content (Table 1).

Table 2. Parameters for defining the HF content compatible with EC8 spectrum (Giaralis & Spanos 2012)

High-frequency content compatible with EC8 spectrum (PGA= 0.36g; Soil B; damping ratio 5%)	$a_{HF}(t)$	$C_{HF} = 0.18 \text{ (m/s}^{2.5}\text{)}$ $b = 0.58 \text{ (s}^{-1}\text{)}$
	$G_{HF}(\omega)$	$\zeta_f = 0.90$
		$\omega_f = 2.33 \text{ (rad/s)}$ $\zeta_g = 0.78$ $\omega_g = 10.73 \text{ (rad/s)}$

Sample realizations compatible with the two PLGM processes and the pulse-free processes are shown in Figure 10. The LF content introduced is not readily discernible in the acceleration traces, however, its effect on structural responses is detrimental for periods longer than 1s, as shown in the elastic response spectra (200 realizations) shown in Figure 11.

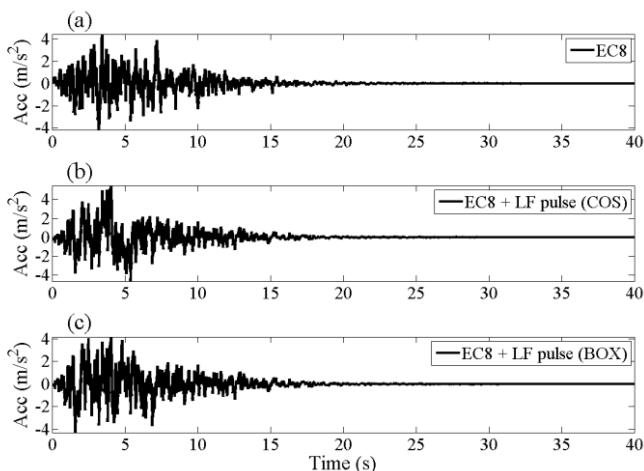


Figure 10 Acceleration samples compatible with EC8: pulse-free (a) and with added pulses (b, c).

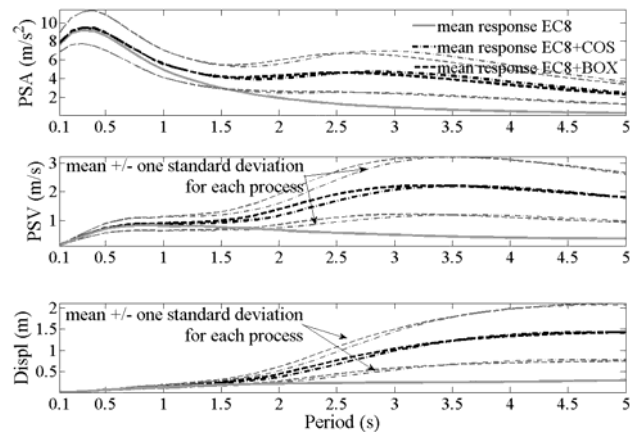


Figure 11 Statistics of elastic response spectral ordinates of the EC8 compatible processes (Tables 1 and 2)- 200 realizations

6 CONCLUDING REMARKS

A non-separable non-stationary stochastic model for representing pulse-like ground motions (PLGMs) has been proposed. It is defined parametrically as a sum of uncorrelated amplitude modulated stationary stochastic processes, representing separately the low frequency (LF) content dominated by the presence of “pulses” (low frequency high energy components) from the high frequency (HF) content. The attractive feature of the model is that it accounts for the narrow-band LF content of PLGMs in a stochastic context as it is commonly considered for the HF content of GMs. In fact, it is amenable to be represented by an evolutionary power spectrum and, thus, it can be readily used as input for stochastic dynamics analyses such as in statistical linearization techniques. Further, it only requires standard methods for spectrum compatible simulation of stationary stochastic processes to yield artificial PLGMs used as input for response history kinds of analyses.

The HF content has been herein represented by a uniformly modulated Clough-Penzien spectral shape, though physics-based seismological models can alternatively be used (e.g. Boore 2003). Two different spectral shapes have been considered for representing the LF content. Pertinent numerical data presented indicate that these shapes have insignificant influence on record-to-record variability of pulse shapes and on the statistical attributes of linear and non-linear peak spectral ordinates. These data involve the consideration of large ensembles of (artificial) PLGMs compatible with the proposed model whose parameters have been calibrated against a specific recorded PLGM. Furthermore, the applicability of the model to yield pulse-like response spectrum compatible accelerograms have been demonstrated by adopting appropriately defined HF stochastic processes compatible in the mean sense with the EC8 response spectrum (Giaralis & Spanos 2012). In this respect, the proposed model might be a valid alternative to represent the seismic action by

means of PLGM spectrum matched accelerograms which is an issue of current concern to the earthquake engineering community (NIST 2011).

Overall, the herein reported numerical results demonstrate the usefulness of the model to generate artificial PLGMs for elastic and inelastic analysis in the case of limited availability of recorded PLGMs. Further numerical work is warranted to demonstrate the applicability of the model to represent PLGMs for various scenario earthquakes by judicious parameter calibration against databanks of field recorded PLGMs and incorporation of predictive relationships for pulse characteristics.

REFERENCES

- Alavi, B. & Krawinkler, H. 2001. Effects of near-fault ground motions on frame structures, *Report no. 131, Department of Civil and Environmental Engineering, Stanford University, California*.
- Baker, J.W. 2007. Quantitative classification of near-fault ground motions using wavelet analysis. *Bulletin of the Seismological Society of America* 97:1486-1501.
- Bogdanoff, J.L., Goldberg, J.E. & Bernard, M.C. 1961. Response of a simple structure to a random earthquake-type disturbance. *Bulletin of the Seismological Society of America* 51:293-310.
- Boore, D.M. 2003. Simulation of ground motion using the stochastic method. *Pure and Applied Geophysics* 160:635-676.
- CEN, 2004. Eurocode 8: Design of Structures for Earthquake Resistance-Part 1: General Rules, Seismic Actions and Rules for Buildings. *EN 1998-1: 2004, Comité Européen de Normalisation, Brussels*.
- Clough, R. & Penzien, J. 1993. *Dynamics of structures, second edition*. New York:McGraw-Hill.
- Conte, J.P. & Peng B.F. 1997. Fully nonstationary analytical earthquake ground-motion model. *Journal of Engineering Mechanics ASCE* 123:15-24.
- Dabaghi, M., Rezaeian, S. & Der Kiureghian, A. 2011. Stochastic simulation of near-fault ground motions for specified earthquake and site characteristics. *Proceedings of the 11th International Conference on Applications of Statistics and Probability in Civil Engineering, Zürich, Switzerland*, pp: 2498-2505.
- Dickinson, B.W. & Gavin, H.P. 2011. Parametric statistical generalization of uniform-hazard earthquake ground motions. *Journal of Structural Engineering* 137:410-422.
- Dugundji, J. 1958. Envelopes and pre-envelopes of real waveforms. *Information Theory, IRE Transactions on* 4:53-57.
- Fu, Q. & Menun, C. 2004. Seismic-environment-based simulation of near-fault ground motions. *13th World Conference on Earthquake Engineering, Vancouver, B.C., Canada*, no. 322, 15pp.
- Giaralis, A. & Spanos, P.D. 2009. Wavelet-based response spectrum compatible synthesis of accelerograms - Eurocode 8 application (EC8). *Soil Dynamics and Earthquake Engineering* 29: 219-235.
- Giaralis, A. & Spanos, P.D. 2012. Derivation of response spectrum compatible non-stationary stochastic processes relying on Monte Carlo-based peak factor estimation. *Earthquakes and Structures* 3:581-609.
- Giaralis, A. & Lungu, A. 2012. Assessment of wavelet-based representation techniques for the characterization of stochastic processes modeling pulse-like strong ground motions. *Proceedings of the 6th International ASRANet Conference for Integrating Structural Analysis, Risk and Reliability, London*.
- He, W. & Agrawal, A.K. 2008. Analytical model of ground motion pulses for the design and assessment of seismic protective systems. *Journal of Structural Engineering* 134: 1177-1188.
- Lai, S.P. 1982. Statistical characterization of strong ground motions using power spectral density function. *Bulletin of Seismological Society of America* 72(1):259-274.
- Mavroedidis, G. & Papageorgiou, A.S. 2003. A mathematical representation of near-fault ground motions. *Bulletin of Seismological Society of America* 93:1099-1131.
- Moustafa, A. & Takewaki, I. 2010. Deterministic and probabilistic representation of near-field pulse-like ground motion. *Soil Dynamics and Earthquake Engineering*, 30:412-422.
- NIST GCR 11-917-15 2011. Selecting and scaling earthquake ground motions for performing response history analyses. *National Institute of standards and technology, US Department of Commerce*.
- Priestley, M.B. 1965. Evolutionary spectra and non-stationary processes. *Journal of the Royal Statistical Society* 27(B):204-237.
- Sehhati, R., Rodriguez-Marek, A., ElGawady, M. & Cofer, W.F. 2011. Effects of near-fault ground motions and equivalent pulses on multi-story structures. *Engineering Structures* 33: 767-779.
- Shinozuka, M. & Deodatis, G. 1991. Simulation of stochastic processes by spectral representation. *Applied Mechanics Reviews* 44:191-204.
- Spanos, P.D. & Vargas Loli, L.M. 1985. A statistical approach to generation of design spectrum compatible earthquake time histories. *Soil Dynamics and Earthquake Engineering* 4:2-8.
- Spanos, P.D. & Zeldin, B.A. 1998. Monte Carlo treatment of random fields: a broad perspective. *Applied Mechanics Reviews* 51:219-37.
- Spanos, P.D. & Failla, G. 2004. Evolutionary spectra estimation using wavelets. *Journal of Engineering Mechanics*, 130(8):952-960.
- Spanos, P.D. & Kougiumtzoglou, I.A. 2011. Harmonic wavelets based statistical linearization for response evolutionary power spectrum determination. *Probabilistic Engineering Mechanics* 27:57-68.
- Spanos, P.D., Giaralis, A. & Politis, N.P. 2007. Time-frequency representation of earthquake accelerograms and inelastic structural response records using the adaptive chirplet decomposition and empirical mode decomposition. *Soil Dynamics and Earthquake Engineering* 27:675-689.
- Spanos, P.D., Giaralis, A. & Jie, L. 2009. Synthesis of accelerograms compatible with the Chinese GB 50011-2001 design spectrum via harmonic wavelets: artificial and historic records. *Earthquake Engineering and Engineering Vibrations* 8:189-206.
- Taflanidis, A.A. & Jia, G. 2011. A simulation-based framework for risk assessment and probabilistic sensitivity analysis of base-isolated structures. *Earthquake Engineering and Structural Dynamics* 40:1629-1651.
- Trifunac, M.D. & Brady, A.G. 1975. A Study on the duration of strong earthquake ground motion. *Bulletin of the Seismological Society of America*, 65: 581-626.
- Vassiliou, M.F. & Makris, N. 2011. Estimating time scales and length scales in pulselike earthquake acceleration records with wavelet analysis. *Bulletin of the Seismological Society of America* 101:596-618.
- Worden, K. 1990. Data processing and experiment design for the restoring force surface method, part I: integration and differentiation of measured time data. *Mechanical Systems and Signal Processing* 4:295-319.